Y. Fan, W. Jing, F. Bernelli-Zazzera
Nonlinear Tracking Differentiator Based Prescribed Performance Control for Space Manipulator
International Journal of Control, Automation, and Systems, Published online 11/02/2023
doi:10.1007/s12555-021-0288-5

Nonlinear Tracking Differentiator based Prescribed Performance Control for Space Manipulator

Yidi Fan*, Wuxing Jing, and Franco Bernelli-zazzera

Abstract: A low-complexity prescribed performance controller is proposed for motion tracking control of a space manipulator in this paper. First of all, a prescribed-time prescribed performance function is designed. Based on the function, the proposed controller is capable of guaranteeing the system transient and steady-state control performances satisfy the prescribed boundary constraints. Moreover, all tracking errors converge to stability domains before the user-defined settling time. A nonlinear tracking differentiator based on a hyperbolic sine function is adopted to estimate the derivatives of joint angles and reconstruct the angular velocity for the controller, which lowers hardware requirements for the controlled system to a certain extent. Without any time-consuming operations and model information, the proposed control scheme has a superiority in low computation complexity and robustness against model uncertainties. With the Lyapunov theory, the prescribed-time stability within prescribed performances of the closed-loop has been rigorously proven. Numerical simulation and the comparison with the traditional prescribed performance control demonstrates the effectiveness and superior performances of the proposed control scheme.

Keywords: Prescribed performance control, prescribed-time stability, space manipulator, motion tracking control, tracking differentiator.

1. INTRODUCTION

Considerable developments of on-orbit service has been witnessed with the sharply increasing number of launched satellites, where space manipulators play a significant role for on-orbit assembly, object inspection, deorbiting of space debris [1-3] and retrieval of malfunctioning satellites [4,5]. In such space missions, the trajectory tracking capability is a direct practical important issue, where accuracy and transient and steady state performance of the closed-loop system is of outmost significance [6,7]. In general, trajectory tracking controllers were mainly designed based on computed torque, inverse dynamic and passivity-based methods [7-9], which need the knowledge of full exact dynamic models. However, model uncertainties bring an obstacle for handling this issue but appear in most cases. For instance, the control of a space robot after capturing a non-cooperative target is a challenging task as the dynamic model of the combination is always unknown [10,11]. In this case, approximation has been employed in manipulator tracking controllers, such as adaptive control and neural network control [12,13]. But these approximation methods require to guarantee beforehand that the system state is restricted to the compact set where the approximation capability hold, which is a tedious task because the usual means is regulating the control parameters and initial parameter estimates to attain the goal. As a consequence, these model-based controllers are very dependent on the complexity and uncertainty of dynamic models, and they are computationally demanding. Thus it is valuable to design model-free controllers for space manipulators, capable of not only increasing the applicability as well as robustness against model uncertainties but also lowering the computation requirement.

Proportional-Integration-Derivative (PID) control method, which is a typical representative of model-free method, has been proved to be capable of stabilizing manipulator systems based on effective adoption of the passivity property [9]. The asymptotic stability of the PID controller for a robot joint angles control problem has been established in a global sense [14] and in semi-global sense [15] by integrating a combined error composed of joint angle errors and angular velocities. In Ref. [16], a PD controller is designed to maintain the

This work was supported by National Natural Science Foundation of China (Grant No. 11572097), and Aerospace Science and Technology Innovation Foundation of China (Grant No. 6141B06030201).

Yidi Fan and Wuxing Jing are with the Department of Aerospace Engineering, Harbin Institute of Technology, 92 West Dazhi Street, Nangang Dist., Harbin, 150001, China (e-mail: fanyidi@hit.edu.cn, jingwuxing@hit.edu.cn). Franco Bernelli-Zazzera is with the Department of Aerospace Science and Technology, Politecnico di Milano, 34 Via La Masa, Milan, 20156, Italy (franco.bernelli@polimi.it). * Corresponding author.

stability of the robot system after the space capture. Although it has been shown that PID controller can guarantee that the tracking error is uniformly ultimate bounded by selecting appropriate control gains, too large gains have an impact on the performance of the closed-loop system directly [17,18]. Attempting to improve the closed-loop system performance, PID gain tuning procedures is presented in Ref. [19] and some advanced methods such as sliding mode control and fuzzy neural network control are introduced Refs. [12,20,21], whereas they all require a prior knowledge of the dynamic model. Furthermore, currently, robotic systems adopt lightweight and flexible materials, embedded sensors and actuators, which make the nonlinear inertia and couplings among the joints become more and more dominant and influential in system performance [22]. In this case, simple PID controller is insufficient to achieve high performance and model-based controllers become fairly complicated and time-consuming. In addition, the accurate angular velocity is sometimes difficult to be achieved from the measurement devices in certain cases for power availability, limited sensing and costs. An approximate angular velocity achieved by the difference between joint angles at adjacent times is usually utilized in practice as a substitute, which is seriously influenced by bandwidth, transmission rate and noise and limit the performance of the controller [23,24]. The above problem imposes limits on the direct application of the full-state-based control scheme.

Most papers on manipulator control problems focus on the stability issue rather than the transient and steady state performance of the closed-loop system, where the performance usually relies on tuning the control parameters, which is a dreary task. In some practical space missions, for example in on-orbit assembly, it is important to control the time attribute of tracking errors since undesirable overshoot may cause damage to assembly units [25]. Prescribed performance control (PPC) is proposed for a variety of uncertain nonlinear systems, by introducing a performance function and an error transformation, to guarantee the convergence of the tracking error to a predefined arbitrarily small residual set, with the convergence rate more than a predefined value and the maximum overshoot less than a sufficiently small one [26-28]. A robust inertia-free attitude takeover control scheme, guaranteeing the prescribed transient and steady-state performance of the closed-loop system, is designed for the postcapture combined spacecraft in [29]. The idea of error transformation extract from [26] has been adopted in robot control problems [30,31]. Specifically, a model-based prescribed performance adaptive controller for the force/position tracking of robot is proposed in Ref. [30]. In Ref. [32], funnel control is utilized to achieve prescribed performance of a robot system output by introducing an auxiliary state consisting of the joint angle and angular velocity tracking errors. The prescribed performance of the auxiliary state, however, does not imply that either joint angle or angular velocity errors are confined within pre-specified boundaries. Authors in Ref. [33] design a model-free controller for a manipulator to guarantee prescribed performance specifications for both joint angle and angular velocity tracking errors, where the accurate measurement of joint angular velocity is a necessary and the system settling time cannot be guaranteed in advance. To the best of authors' knowledge, there does not exist any model-free continuous control scheme that achieves prescribed time and prescribed performance of both joint angle and angular velocity tracking errors for space manipulators.

In this paper, based on a nonlinear tracking differentiator (TD), a low-complexity model-free controller guaranteeing both prescribed time and prescribed performance is proposed for motion tracking control of a space manipulator. The contributions of this paper are as follows:

1) This paper proposes a low-complexity prescribed-time prescribed-performance control (PTPPC) method for space manipulators, which requires no time-consuming operations (iterative computation, for instant) and thus can be utilized online in space missions.

2) The traditional prescribed performance function is extended to prescribed-time prescribed-performance function which is able to guarantee that not only the system transient and steady-state control performances satisfy the prescribed boundary constraints but also tracking errors converge to stability domains before the user-defined settling time.

3) The proposed control scheme is partial-state-based with a hyperbolic-sine-function-based tracking differentiator. This lowers hardware requirements for the controlled system to a certain extent and is suitable for a wide range of applications, since the accurate angular velocity is sometimes difficult to be inferred from the measurement devices in certain cases for power availability, limited sensing or costs.

4) The control scheme designed in this note is model-free in the sense that it does not incorporate either any information regarding the space manipulator model or approximation computation, which increases its applicability as well as robustness against model uncertainties. Moreover, it is an easy task to select the controller gain because adjusting them to generate reasonable input torques is the only consideration.

The remainder of this paper is organized as follows. The manipulator control problem is formulated in Section II. A nonlinear tracking differentiator and a low-complexity model-free controller utilizing prescribed-time prescribed-performance functions are designed in Section III. A stability analysis based on the Lyapunov theory is presented as well. Numerical simulation results are presented in Section IV to demonstrate the effectiveness of the control method. The conclusions in Section V end the paper.

2. PROBLEM FORMULATION

Consider a servicing spacecraft equipped a 6-DOF manipulator without kinematic singularities. One may consider a redundant manipulator in order to actively avoid singularities via a redundancy resolution algorithm. The dynamics of the whole system is given by the following general equation:

$$\begin{bmatrix} \boldsymbol{M}_b & \boldsymbol{M}_{bm} \\ \boldsymbol{M}_{bm}^T & \boldsymbol{D} \end{bmatrix} \begin{bmatrix} \ddot{\boldsymbol{\Phi}} \\ \ddot{\boldsymbol{q}} \end{bmatrix} + \begin{bmatrix} \boldsymbol{c}_b \\ \boldsymbol{c}_m \end{bmatrix} = \begin{bmatrix} \boldsymbol{f} \\ \boldsymbol{\tau} \end{bmatrix} + \begin{bmatrix} \boldsymbol{d}_b \\ \boldsymbol{d}_m \end{bmatrix} \tag{1}$$

where $\dot{\boldsymbol{\Phi}}$ is the generalized velocity of the spacecraft base consisting of the linear and angular velocities, and $\boldsymbol{q}$ is the joint angle position of the manipulator. $\boldsymbol{M}_b$ and $\boldsymbol{D}$ denote inertia matrices of the spacecraft base and manipulator, respectively, while $\boldsymbol{M}_{bm}$ denotes the coupling inertia matrix between them. $\boldsymbol{c}_b$ and $\boldsymbol{c}_m$ denote nonlinear terms, containing Coriolis and centrifugal forces, acting on the spacecraft base and manipulator, respectively. $\boldsymbol{f}$ represents the generalized force imposed on the spacecraft base and $\boldsymbol{\tau}$ stands for the controls vector of joints. $\boldsymbol{d}_b$ and $\boldsymbol{d}_m$ denote external disturbances acting on the spacecraft base and manipulator, respectively, which can be assumed as continuous bounded terms according to practice.

In this paper, we consider a manipulator and assume that it does not experience kinematic singularities. Nonetheless, one may consider a redundant manipulator in order to actively avoid singularities via a redundancy resolution algorithm. Because we are interested in only controlling the motion of the manipulator, it can be assumed that the torque is applied to the spacecraft base by the actuators of its attitude control system to remain stable. Then, the dynamics of the manipulator can be written as

$$\boldsymbol{D}\ddot{\boldsymbol{q}} + \boldsymbol{C}\dot{\boldsymbol{q}} + \boldsymbol{\Delta} = \boldsymbol{\tau} \tag{2}$$

where $\boldsymbol{D}$ is a positive definite and symmetric matrix related to $\boldsymbol{q}$. $\boldsymbol{c}_m = \boldsymbol{C}\dot{\boldsymbol{q}}$ where $\boldsymbol{C}$ is related to $\boldsymbol{q}$ and $\dot{\boldsymbol{q}}$. $\boldsymbol{\Delta}$ denotes the disturbance term, including external disturbances $\boldsymbol{d}_m$ and $\boldsymbol{M}_{bm}^T\ddot{\boldsymbol{\Phi}}$ which is the disturbance that the base exerts on the manipulator. This term is bounded when the base keeps stable, and will be tackled with the robust controller to be designed. For simplicity hereafter, we define that $\|\cdot\|$ denotes the Euclidean norm, and $\lambda_{\min}(\cdot)$ and $\lambda_{\max}(\cdot)$ denote the minimum and maximum eigenvalue, respectively. Some critical properties of Eq.(2) are introduced as follows.

Lemma 1 [34]**:** The matrices $\boldsymbol{D}$ and $\boldsymbol{C}$ satisfy the following properties:

1) The matrix $\boldsymbol{D}$ satisfies the inequality $0 < \lambda_{\min}(\boldsymbol{D}^{-1}) \le \|\boldsymbol{D}^{-1}\| \le \lambda_{\max}(\boldsymbol{D}^{-1})$.

2) The matrix $\boldsymbol{C}$ is bounded when all joint angle positions and velocities are bounded.

3) The matrix $\dot{\boldsymbol{D}} - 2\boldsymbol{C}$ is skew-symmetric, that is $\boldsymbol{s}^{\mathrm{T}}(\dot{\boldsymbol{D}} - 2\boldsymbol{C})\boldsymbol{s} = \boldsymbol{0}$, $\forall \boldsymbol{s} \in \mathbb{R}^n$.

Without loss of generality, the reference signals satisfy the following assumption.

Assumption 1: The reference joint angle velocity $\dot{\boldsymbol{q}}_r$ and its derivative $\ddot{\boldsymbol{q}}_r$ are both bounded and continuous over *t*. More specifically, $\|\dot{\boldsymbol{q}}_r\| \le l_{\dot{q}r}$ and $\|\ddot{\boldsymbol{q}}_r\| \le l_{\ddot{q}r}$ with two bounded unknown nonnegative constants $l_{\dot{q}r}$ and $l_{\ddot{q}r}$.

3. PRESCRIBED-TIME PRESCRIBED-PERFORMANCE CONTROL SCHEME DESIGN

In this section, a low-complexity model-free PTPPC control scheme based on prescribed-time prescribed-performance functions is presented and its closed-loop performance is analyzed with the Lyapunov theory.

3.1. Prescribed-time prescribed-performance function

Prescribed performance is achieved if a generic tracking error $e \in \mathbb{R}$ satisfies the following inequality:

$$\underline{\alpha}(t) \le e \le \bar{\alpha}(t), \quad \forall t \ge 0 \tag{3}$$

where the performance boundaries $\underline{\alpha}(t)$ and $\bar{\alpha}(t)$ are continuous, bounded and positive time functions.

Defining a constant $\delta \in (0,1)$ denoting the maximum overshoot index and a continuous, bounded and positive time function $\alpha(t)$, the performance boundaries in Eq. (3) can be given by

$$\begin{cases} \underline{\alpha}(t) = -\delta\alpha(t), \quad \bar{\alpha}(t) = \alpha(t), & \text{if } e(0) \ge 0 \\ \underline{\alpha}(t) = -\alpha(t), \quad \bar{\alpha}(t) = \delta\alpha(t), & \text{else.} \end{cases} \tag{4}$$

And the transient and steady state performances of the tracking error *e* are bounded in the open set *D*, i.e. for $\forall t \ge 0$, one has

$$e \in D \tag{5}$$

where

$$D = \begin{cases} (-\delta\alpha(t), \alpha(t)), & \text{if } e(0) \ge 0 \\ (-\alpha(t), \delta\alpha(t)), & \text{else.} \end{cases}$$

The prescribed-time prescribed-performance function is designed as

$$\alpha(t) = \begin{cases} \left(\frac{T-t}{T}\right)^{\frac{1}{1-\gamma}}(\alpha^0 - \alpha^T) + \alpha^T, & \text{if } 0 \le t \le T \\ \alpha^T, & \text{else} \end{cases} \tag{6}$$

where $\gamma \in (0,1)$ determines the decrease rate of the performance function before the prescribed time *T*. α^0 represents the initial value of $\alpha(t)$, which should be selected to satisfy prescribed stability domain at $t = 0$ in applications. α^T represents the maximum allowable value of the tracking error at the steady state. The piecewise performance function is able to not only confine tracking errors to prescribed performance boundaries but also enable them to converge to stability domains before the user-defined settling time *T*. An illustration of an error evolution with the prescribed-time prescribed-performance is shown in Fig. 1, where the vertical dotted lines denote the prescribed time *T*. It should be noted that for any given prescribed time *T* and $\alpha^0 > \alpha^T > 0$, $\alpha(t)$ is monotone decreasing when $0 \le t \le T$ and continuous for $t \ge 0$. Its first-order time derivative $\dot{\alpha}(t)$ is continuous when $t \ge 0$ as well.

Defining a normalized tracking error

$$\theta(t) = \frac{e(t)}{\alpha(t)} \tag{7}$$

and the error transformation mapping

$$\eta(t)=\mu(\theta)=\begin{cases}\ln\dfrac{\delta+\theta}{\delta(1-\theta)}, & \text{if } e(0)\geq 0\\ \ln\dfrac{\delta(1+\theta)}{\delta-\theta}, & \text{else}\end{cases} \tag{8}$$

which is apparently a smooth, strictly increasing and invertible function, the prescribed performance inequality Eq. (3) can be expressed as

$$\theta\in\Omega \tag{9}$$

where

$$\Omega=\begin{cases}(-\delta,1), & \text{if } e(0)\geq 0\\ (-1,\delta), & \text{else}\end{cases},\ \forall t\geq 0\,.$$

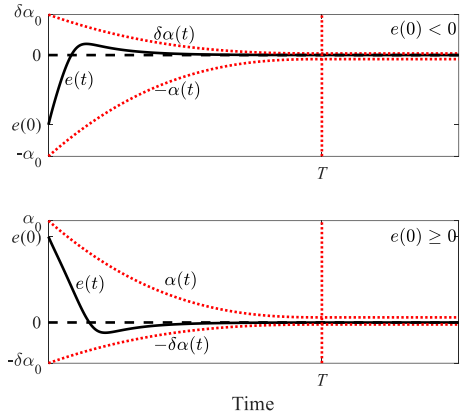

Fig. 1. Illustration of an error evolution with the prescribed-time prescribed-performance.

Differentiating Eq.(8) with respect to θ and time respectively, one can obtain the following properties concerning the error transformation mapping $\mu(\cdot)$.

$$\frac{\partial\mu(\theta)}{\partial\theta}=\begin{cases}\dfrac{1+\delta}{(\delta+\theta)(1-\theta)}, & \text{if } e(0)\geq 0\\ \dfrac{1+\delta}{(\delta-\theta)(1+\theta)}, & \text{else,}\end{cases} \tag{10}$$

$$\frac{\partial\mu(\theta)}{\partial\theta}\in\left[\frac{4}{1+\delta},+\infty\right), \tag{11}$$

$$\rho(\theta)=\frac{\mu(\theta)}{\theta}\in\left[\frac{4}{1+\delta},+\infty\right) \tag{12}$$

where $\rho(\theta)$ is a continuous function in its domain of definition (9) and its continuity in the singular point $\theta=0$ can be easily proved by the L'Hospital's rule.

$$\dot\eta(t)=R[\dot e(t)+He(t)] \tag{13}$$

where

$$R=\frac{\partial\mu(\theta)}{\partial\theta}\frac{1}{\alpha(t)}\in\left[\frac{4}{(1+\delta)\alpha^0},+\infty\right),$$

$$H=-\frac{\dot\alpha(t)}{\alpha(t)}\geq 0\,.$$

The satisfaction of the prescribed performance boundary Eq.(5) concerning the tracking error $e(t)$ can be transformed to the boundedness of the error transformation mapping $\eta(t)$. In fact, given $|\eta(t)|\leq\varepsilon$, where ε is a positive constant, the normalized tracking error $\theta(t)$ is confined to a compact set $J\subset\Omega$, where

$$J=[\mu^{-1}(-\varepsilon),\mu^{-1}(\varepsilon)] \tag{14}$$

which implies that the tracking error $e(t)$ evolves strictly within the prescribed performance boundary Eq.(5).

To summarize, selecting α_0 such that Eq.(5) is satisfied at $t=0$, the error transformation mapped state $\eta(t)$ is initially well defined to be finite. Then, designing a control law that restricts the boundedness of $\eta(t)$ for $t\geq 0$ thus arrives Eq.(5).

3.2. Tracking differentiator

The joint angles $\boldsymbol{q}$ as well as the angular velocity $\dot{\boldsymbol{q}}$ in the nonlinear system (2) are the key information for control design. However, the accurate angular velocity is sometimes difficult to be achieved from the sensors in certain cases for power availability, limited sensing and costs, which imposes limits on the direct application of the full-state-based control scheme. In this paper, to address this problem, we employ a hyperbolic-sine-function-based TD to estimate the derivatives of joint angles and reconstruct the angular velocity for the controller.

The TD is developed as follows:

$$\begin{cases}\dot y_i(t)=\omega_i(t)\\ \dot\omega_i(t)=-p_{0i}^2(p_{1i}\sinh(s_{1i}(y_i(t)-q_i(t)))\\ \qquad\qquad +p_{2i}\sinh(s_{2i}\omega_i(t)/p_{0i}))\end{cases} \tag{15}$$

where p_{0i}, p_{1i}, p_{2i}, s_{1i} and s_{2i} are positive constants to be designed. y_i is the estimation of q_i and ω_i is the estimation of $\dot q_i$, $i=1,\cdots,6$.

Proof: To prove the system (15) is asymptotical stable, we consider a following representative system where the subscript *i* is dropped.

$$\begin{cases}\dot z_1(t)=z_2(t)\\ \dot z_2(t)=-p_0^2p_1\sinh(s_1z_1(t))-p_0^2p_2\sinh(s_2z_2(t))\end{cases} \tag{16}$$

where $z_1(t)=y(t)-q(t)$ and $z_2(t)=\omega(t)/p_0$.

Let us define a Lyapunov function candidate as

$$V_z=\int_0^{z_1}p_0^2p_1\sinh(s_1\varsigma)d\varsigma+\frac{1}{2}z_2^2\,. \tag{17}$$

Owing to the odd function $\sinh(\cdot)$, one has the derivative of V_z:

$$\dot V_z=-p_0^2p_2z_2(t)\sinh(s_2z_2(t))\leq 0\,. \tag{18}$$

In the light of the definition of weak convergence, the system (16) is asymptotical stable at the origin. Invoking Lemma 1 in [35] thus arrives that for a bounded and integrable function $q(t)$ and a constant t_1, one gets

$$\lim_{p_0\to\infty}\int_0^{t_1}|z_1(t)-q(t)|dt=0\,. \tag{19}$$

This is the end of proof. □

Thus one can obtain that the estimation error denoted by $\boldsymbol{e}_{est}(t)=[e_{est,1}(t),\cdots,e_{est,6}(t)]^{\mathrm{T}}$ satisfies $\|\boldsymbol{e}_{est}(t)\|\leq l_{est}$ for $t\geq 0$ and its derivative $\dot{\boldsymbol{e}}_{est}(t)$ is bounded as well, where $e_{est,i}(t)=\omega_i(t)-\dot q_i(t)$, $i=1,\cdots,6$, and l_{est} is a unknown bounded constant.

Remark 1: The design parameters p_{0i}, p_{1i}, p_{2i}, s_{1i} and s_{2i} have different effects on the tracking and differentiation performance of the TD in (15). The relationship between the state z_1 and each parameters are shown in Figs 2-3. Obviously, the larger p_{0i}, p_{1i} and s_{1i} and smaller p_{2i} and s_{2i} bring higher convergence rate and accuracy, and vice versa. Yet too large p_{1i} and s_{1i} and too small p_{2i} and s_{2i} may lead to an undesired overshoot.

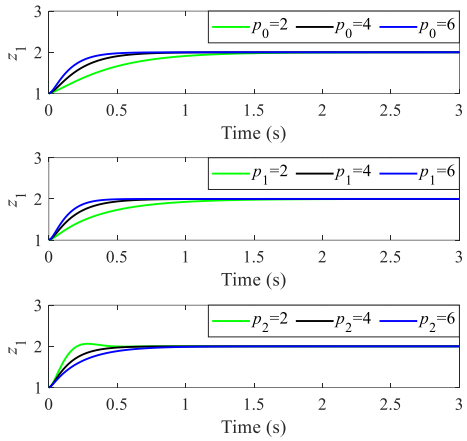

Fig. 2. Time histories of z_1 for different parameters.

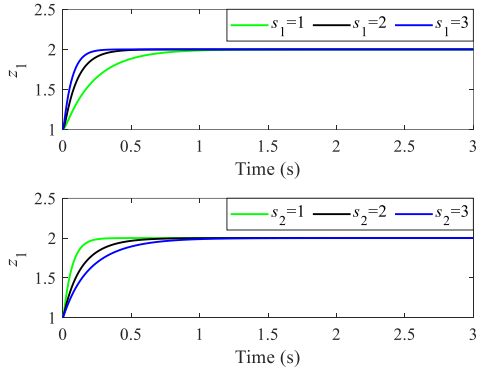

Fig. 3. Time histories of z_1 for different parameters.

3.3. Controller design

The control objective of the tracking control problem in Eq.(2) is to propose a robust controller to ensure that the tracking joint angle error $\tilde{\boldsymbol{q}} = \boldsymbol{q} - \boldsymbol{q}_r$ and angular velocity error $\dot{\tilde{\boldsymbol{q}}} = \dot{\boldsymbol{q}} - \dot{\boldsymbol{q}}_r$ are capable of reaching their prescribed stability regions before the prescribed time T which can be predefined by users. Both of the transient and steady state performances can be guaranteed during the convergence process.

Since the angular velocity $\dot{\boldsymbol{q}}(t)$ is estimated as $\boldsymbol{\omega}(t) = [\omega_1(t), \cdots, \omega_6(t)]^{\mathrm{T}}$ by the TD in Eq.(15), we define the tracking angular velocity error $\tilde{\boldsymbol{\omega}}(t) = \boldsymbol{\omega}(t) - \dot{\boldsymbol{q}}_r(t)$. Thus a nonlinear auxiliary state $\boldsymbol{x}(t) = [x_1(t), \cdots, x_6(t)]^{\mathrm{T}}$ is defined as follows:

$$\boldsymbol{x}(t) = \xi \tilde{\boldsymbol{q}}(t) + \tilde{\boldsymbol{\omega}}(t) \tag{20}$$

where ξ is a design positive constant.

To proceed, in (21) and (22), define two prescribed-time prescribed-performance functions $\alpha_{qi}(t)$ and $\alpha_{xi}(t)$ in the form of Eq.(6) with identical γ and T to impose on $\tilde{q}_i$ and x_i, $i = 1, \cdots, 6$, respectively. We have the boundary constraints in (23) and (24).

$$\alpha_{qi}(t) = \begin{cases} (\dfrac{T-t}{T})^{\frac{1}{1-\gamma}} (\alpha_{qi}^0 - \alpha_{qi}^T) + \alpha_{qi}^T, & \text{if } 0 \le t \le T \\ \alpha_{qi}^T, & \text{else,} \end{cases} \tag{21}$$

$$\alpha_{xi}(t) = \begin{cases} (\dfrac{T-t}{T})^{\frac{1}{1-\gamma}} (\alpha_{xi}^0 - \alpha_{xi}^T) + \alpha_{xi}^T, & \text{if } 0 \le t \le T \\ \alpha_{xi}^T, & \text{else,} \end{cases} \tag{22}$$

$$\begin{cases} -\delta\alpha_{qi}(t) < \tilde{q}_i(t) < \alpha_{qi}(t), & \text{if } \tilde{q}_i(0) \ge 0 \\ -\alpha_{qi}(t) < \tilde{q}_i(t) < \delta\alpha_{qi}(t), & \text{else,} \end{cases} \tag{23}$$

$$\begin{cases} -\delta\alpha_{xi}(t) < x_i(t) < \alpha_{xi}(t), & \text{if } x_i(0) \ge 0 \\ -\alpha_{xi}(t) < x_i(t) < \delta\alpha_{xi}(t), & \text{else} \end{cases} \tag{24}$$

where α_{qi}^0, α_{qi}^T, α_{xi}^0 and α_{qi}^T denote the initial values and maximum allowable values of the $\tilde{\boldsymbol{q}}$ and $\boldsymbol{x}$, respectively. Then we have $\boldsymbol{\alpha}_q = [\alpha_{q1}, \cdots, \alpha_{q6}]^{\mathrm{T}}$ and $\boldsymbol{\alpha}_x = [\alpha_{x1}, \cdots, \alpha_{x6}]^{\mathrm{T}}$.

Define the normalized tracking errors

$$\theta_{qi}(t) = \frac{\tilde{q}_i(t)}{\alpha_{qi}(t)}, \tag{25}$$

$$\theta_{xi}(t) = \frac{x_i(t)}{\alpha_{xi}(t)} \tag{26}$$

where $i = 1, \cdots, 6$,and transform them into mapped states $\eta_{qi}(t)$ and $\eta_{xi}(t)$ via Eq.(8). Differentiating $\eta_{qi}(t)$ and $\eta_{xi}(t)$ yield that

$$\dot{\eta}_{qi}(t) = R_{qi}[\dot{\tilde{q}}_i(t) + H_{qi}\tilde{q}_i(t)], \tag{27}$$

$$\dot{\eta}_{xi}(t) = R_{xi}[\dot{x}_i(t) + H_{xi}x_i(t)] \tag{28}$$

where $i = 1, \cdots, 6$, and the definitions of R_{qi}, H_{qi}, R_{xi} and H_{xi} are similar to R and H in Eq.(13).

Then, we define the following vectors and matrices:

$$\boldsymbol{\theta}_q(t) = [\theta_{q1}(t), \cdots, \theta_{q6}(t)]^{\mathrm{T}},$$
$$\boldsymbol{\theta}_x(t) = [\theta_{x1}(t), \cdots, \theta_{x6}(t)]^{\mathrm{T}},$$
$$\boldsymbol{\eta}_q(t) = [\eta_{q1}(t), \cdots, \eta_{q6}(t)]^{\mathrm{T}},$$
$$\boldsymbol{\eta}_x(t) = [\eta_{x1}(t), \cdots, \eta_{x6}(t)]^{\mathrm{T}},$$
$$\boldsymbol{R}_q = \mathrm{diag}([R_{q1}, \cdots, R_{q6}]^{\mathrm{T}}),$$
$$\boldsymbol{R}_x = \mathrm{diag}([R_{x1}, \cdots, R_{x6}]^{\mathrm{T}}),$$
$$\boldsymbol{H}_q = \mathrm{diag}([H_{q1}, \cdots, H_{q6}]^{\mathrm{T}}),$$
$$\boldsymbol{H}_x = \mathrm{diag}([H_{x1}, \cdots, H_{x6}]^{\mathrm{T}}).$$

Given the system dynamics (2) and subject to boundary constraints (23) and (24), the control law

$$\boldsymbol{\tau} = -\boldsymbol{R}_q\tilde{\boldsymbol{q}} - \boldsymbol{\eta}_q - \boldsymbol{k}_x\boldsymbol{R}_x\boldsymbol{\eta}_x \tag{29}$$

will drive the joint angle error $\tilde{\boldsymbol{q}}$ and angular velocity error $\dot{\tilde{\boldsymbol{q}}}$ to fulfil the control objectives, and the design parameter $\boldsymbol{k}_x$ is a positive diagonal matrix.

Applying the Lyapumov stability theory, a crucial conclusion is derived as follows:

Theorem 1: Consider the tracking control problem in Eq.(2) under Assumption 1, the TD in Eq.(15) and PTPPC in Eq.(29). If the prescribed-time prescribed-performance functions $\alpha_{qi}(t)$ and $\alpha_{xi}(t)$ are selected to satisfy $\alpha_{qi}^0 > |\tilde{q}_i(0)|$ and $\alpha_{xi}^0 > |x_i(0)|$, respectively, ξ meets $\xi > l_{Hq}$, where $l_{Hq} = \max_i(H_{qi})$, the parameters p_{0i}, p_{1i}, p_{2i}, s_{1i} and s_{2i} in TD are appropriately selected and the control parameter $\boldsymbol{k}_x$ is assigned as a proper positive diagonal matrix, the developed control law in (29) guarantees that:

1) The prescribed performance boundary constraints for $\tilde{\boldsymbol{q}}$ and $\boldsymbol{x}$ always hold for $t \geq 0$.

2) The tracking errors $\tilde{q}_i(t)$ and auxiliary states $x_i(t)$, $i = 1, \cdots, 6$ converge to their stability regions D_{qi} and D_{xi} respectively before the prescribed time T, where

$$D_{qi} = \begin{cases} (-\delta\alpha_{qi}^T, \alpha_{qi}^T), & \text{if } \tilde{q}_i(0) \geq 0 \\ (-\alpha_{qi}^T, \delta\alpha_{qi}^T), & \text{else,} \end{cases} \tag{30}$$

$$D_{xi} = \begin{cases} (-\delta\alpha_{xi}^T, \alpha_{xi}^T), & \text{if } x_i(0) \geq 0 \\ (-\alpha_{xi}^T, \delta\alpha_{xi}^T), & \text{else.} \end{cases} \tag{31}$$

3) The joint angular velocity errors $\dot{\tilde{\boldsymbol{q}}}$ remains bounded for $t \geq 0$.

Proof: In the first place, the relationship among the boundedness of $\tilde{\boldsymbol{q}}$, $\boldsymbol{x}$ and $\dot{\tilde{\boldsymbol{q}}}$ is derived.

According to Eq.(20), it can be obtained that

$$\|\dot{\tilde{\boldsymbol{q}}}\| \leq \|\boldsymbol{x}\| + \xi\|\tilde{\boldsymbol{q}}\| + \|\boldsymbol{e}_{est}\|. \tag{32}$$

Owing to $\|\boldsymbol{e}_{est}(t)\| \leq l_{est}$, where l_{est} is a unknown bounded constant, thus if $\boldsymbol{x}$ and $\tilde{\boldsymbol{q}}$ are bounded, the boundedness of $\dot{\tilde{\boldsymbol{q}}}$ is achieved.

In the following, we will prove that the prescribed performance boundary constraints for $\tilde{\boldsymbol{q}}$ and $\boldsymbol{x}$ always hold for $t \geq 0$. The first step is proving that there exists a time interval $[0, t_f)$ so that the state variables $\tilde{q}_i(t)$, $x_i(t)$ and $\dot{\tilde{q}}_i(t)$ converge to their stability regions simultaneously during the interval.

The relative errors $\boldsymbol{\theta}_q$ and $\boldsymbol{\theta}_x$ can be denoted as $\boldsymbol{\theta}_q = \text{diag}^{-1}(\boldsymbol{\alpha}_q)\tilde{\boldsymbol{q}}$ and $\boldsymbol{\theta}_x = \text{diag}^{-1}(\boldsymbol{\alpha}_x)\boldsymbol{x}$, and we define $\boldsymbol{\theta} = [\boldsymbol{\theta}_q^{\mathrm{T}}, \boldsymbol{\theta}_x^{\mathrm{T}}]^{\mathrm{T}}$ and $\boldsymbol{\alpha} = [\boldsymbol{\alpha}_q^{\mathrm{T}}, \boldsymbol{\alpha}_x^{\mathrm{T}}]^{\mathrm{T}}$. Since $\alpha_{qi}(t)$ and $\alpha_{xi}(t)$ satisfy $\alpha_{0,qi} > |\tilde{q}_i(0)|$ and $\alpha_{0,xi} > |x_i(0)|$, respectively, it is obvious to obtain that $\boldsymbol{\theta}(0) \in D_\theta$, where $D_\theta = D_{\theta 1} \times \cdots \times D_{\theta 12}$ and

$$D_{\theta i} = \begin{cases} (-\delta, 1), & \text{if } \theta_i(0) \geq 0 \\ (-1, \delta), & \text{else} \end{cases}, \quad i = 1, \cdots, 12.$$

To continue, the dynamics of the space manipulator can be rewritten in the following form:

$$\begin{aligned} \dot{\boldsymbol{\theta}} &= f(\boldsymbol{\theta}, t) \\ &= \text{diag}^{-1}(\boldsymbol{\alpha}(t))\begin{bmatrix} \dot{\tilde{\boldsymbol{q}}}(t) \\ \dot{\boldsymbol{x}}(t) \end{bmatrix} - \text{diag}^{-1}(\boldsymbol{\alpha}(t))\text{diag}(\dot{\boldsymbol{\alpha}}(t))\boldsymbol{\theta} \end{aligned} \tag{33}$$

where $f(\boldsymbol{\theta}, t) : D_\theta \times \mathbb{R}^+ \to \mathbb{R}^{12}$.

It is obvious that $f(\boldsymbol{\theta}, t)$ is continuous over $t > 0$ and $\boldsymbol{\theta} \in D_\theta$. Besides, $\partial f(\boldsymbol{\theta}, t)/\partial\boldsymbol{\theta}$ is also continuous over $\boldsymbol{\theta} \in D_\theta$. Invoking Lemma 3.2 in [36], $f(\boldsymbol{\theta}, t)$ is locally Lipschitz with respect to $\boldsymbol{\theta}$. Furthermore, we have

$$\begin{aligned} f(\boldsymbol{\theta}(0), t) = \text{diag}^{-1}(\boldsymbol{\alpha}(t))\begin{bmatrix} \dot{\tilde{\boldsymbol{q}}}(0) \\ \dot{\boldsymbol{x}}(0) \end{bmatrix} \\ -\text{diag}^{-1}(\boldsymbol{\alpha}(t))\text{diag}(\dot{\boldsymbol{\alpha}}(t))\boldsymbol{\theta}(0) \end{aligned} \tag{34}$$

where $f(\boldsymbol{\theta}(0), t)$ is a continuous and bounded function over the time interval $[0, +\infty)$, which implies that it is locally integrable related to t. Consequently, exploring Theorem 54 in [37] reaches a conclusion that there exists a time t_f so that $\boldsymbol{\theta}(t)$ remains in the compact set D_θ for all $t \in [0, t_f)$. In other words, the boundary constraints of $\tilde{q}_i(t)$, $x_i(t)$ and $\dot{\tilde{q}}_i(t)$ are satisfied simultaneously in the time interval $[0, t_f)$.

Then, it will be proved that the mapped state $\boldsymbol{\eta}_q$ and $\boldsymbol{\eta}_x$ satisfy the prescribed performance boundary constraints during the time interval $[0, t_f)$.

Taking the derivative of (20), premultiplying by the inertia matrix $\boldsymbol{D}$ both sides of the equation and substituting the nominal form of (2) yields

$$\begin{aligned} \boldsymbol{D}\dot{\boldsymbol{x}} &= \xi\boldsymbol{D}\dot{\tilde{\boldsymbol{q}}} + \boldsymbol{D}\dot{\tilde{\boldsymbol{\omega}}} \\ &= \xi\boldsymbol{D}\dot{\tilde{\boldsymbol{q}}} + \boldsymbol{D}\dot{\boldsymbol{e}}_{est} + \boldsymbol{\tau} - \boldsymbol{D}\ddot{\boldsymbol{q}}_r - \boldsymbol{C}\dot{\boldsymbol{q}}_r - \boldsymbol{C}\dot{\tilde{\boldsymbol{q}}}. \end{aligned} \tag{35}$$

Assign a Lyapunov function V_1 as follows:

$$V_1 = \frac{1}{2}\boldsymbol{x}^{\mathrm{T}}\boldsymbol{D}\boldsymbol{x} + \boldsymbol{\eta}_q^{\mathrm{T}}\tilde{\boldsymbol{q}}. \tag{36}$$

Taking the derivate of V_1, one can obtain

$$\begin{aligned} \dot{V}_1 &= \boldsymbol{x}^{\mathrm{T}}\boldsymbol{D}\dot{\boldsymbol{x}} + \frac{1}{2}\boldsymbol{x}^{\mathrm{T}}\dot{\boldsymbol{D}}\boldsymbol{x} + \boldsymbol{\eta}_q^{\mathrm{T}}\dot{\tilde{\boldsymbol{q}}}_{\tilde{q}} + \tilde{\boldsymbol{q}}^{\mathrm{T}}\dot{\boldsymbol{\eta}}_q \\ &= \boldsymbol{x}^{\mathrm{T}}(\xi\boldsymbol{D}\dot{\tilde{\boldsymbol{q}}} + \boldsymbol{D}\dot{\boldsymbol{e}}_{est} - \boldsymbol{D}\ddot{\boldsymbol{q}}_r - \boldsymbol{C}\dot{\boldsymbol{q}}_r - \boldsymbol{C}\dot{\tilde{\boldsymbol{q}}} + \boldsymbol{\tau}) \\ &\quad + \frac{1}{2}\boldsymbol{x}^{\mathrm{T}}\dot{\boldsymbol{D}}\boldsymbol{x} + \boldsymbol{\eta}_q^{\mathrm{T}}\dot{\tilde{\boldsymbol{q}}}_q + \tilde{\boldsymbol{q}}^{\mathrm{T}}\boldsymbol{R}_q(\dot{\tilde{\boldsymbol{q}}} + \boldsymbol{H}_q\tilde{\boldsymbol{q}}) \\ &= \boldsymbol{x}^{\mathrm{T}}(\boldsymbol{f}_q + \boldsymbol{\tau} + \boldsymbol{\eta}_q + \boldsymbol{R}_q\tilde{\boldsymbol{q}}) + \frac{1}{2}\boldsymbol{x}^{\mathrm{T}}(\dot{\boldsymbol{D}} - 2\boldsymbol{C})\boldsymbol{x} \\ &\quad -\xi\boldsymbol{\eta}_q^{\mathrm{T}}\tilde{\boldsymbol{q}} - \boldsymbol{\eta}_q^{\mathrm{T}}\boldsymbol{e}_{est} - \tilde{\boldsymbol{q}}^{\mathrm{T}}\boldsymbol{R}_q\boldsymbol{e}_{est} - \tilde{\boldsymbol{q}}^{\mathrm{T}}\boldsymbol{R}_q(\xi\boldsymbol{I} - \boldsymbol{H}_q)\tilde{\boldsymbol{q}} \end{aligned} \tag{37}$$

where $\boldsymbol{f}_q = \xi\boldsymbol{D}\dot{\tilde{\boldsymbol{q}}} + \boldsymbol{D}\dot{\boldsymbol{e}}_{est} - \boldsymbol{D}\ddot{\boldsymbol{q}}_r - \boldsymbol{C}\dot{\boldsymbol{q}}_r + \xi\boldsymbol{C}\tilde{\boldsymbol{q}} + \boldsymbol{C}\boldsymbol{e}_{est}$.

According to previous proof, we get that $\tilde{\boldsymbol{q}}$, $\dot{\tilde{\boldsymbol{q}}}$ and $\boldsymbol{x}$ all satisfy their boundary constraints when $t \in [0, t_f)$ and $\boldsymbol{e}_{est}$ and $\dot{\boldsymbol{e}}_{est}$ are bounded if the TD is well designed. Owing to Lemma 1 and the fact that $\|\dot{\boldsymbol{q}}_r\| \leq l_{\dot{q}r}$ and $\|\ddot{\boldsymbol{q}}_r\| \leq l_{\ddot{q}r}$ in Assumption 1, there exists a constant $l_{fq} \geq 0$ such that

$$\left\| \boldsymbol{f}_q \right\| \le l_{fq} . \tag{38}$$

Recalling Lemma 1 and substituting the control law (29), we have

$$\begin{aligned} \dot{V}_1 &= \boldsymbol{x}^{\mathrm{T}} \boldsymbol{D}\dot{\boldsymbol{x}} + \frac{1}{2}\boldsymbol{x}^{\mathrm{T}}\dot{\boldsymbol{D}}\boldsymbol{x} + \boldsymbol{\eta}_q^{\mathrm{T}}\dot{\boldsymbol{\eta}}_{\tilde{q}} \\ &= \boldsymbol{x}^{\mathrm{T}}\boldsymbol{f}_q - \boldsymbol{x}^{\mathrm{T}}\boldsymbol{k}_x\boldsymbol{R}_x\boldsymbol{\eta}_x - \xi\boldsymbol{\eta}_q^{\mathrm{T}}\tilde{\boldsymbol{q}} - \boldsymbol{\eta}_q^{\mathrm{T}}\boldsymbol{e}_{est} - \tilde{\boldsymbol{q}}^{\mathrm{T}}\boldsymbol{R}_q\boldsymbol{e}_{est} \\ &\quad -\tilde{\boldsymbol{q}}^{\mathrm{T}}\boldsymbol{R}_q(\xi\boldsymbol{I} - \boldsymbol{H}_q)\tilde{\boldsymbol{q}} \end{aligned} \tag{39}$$

where $\boldsymbol{I}$ is a unit matrix. Owing to ξ is selected to meet $\xi > \max_i(H_{qi})$, one obtains $\boldsymbol{\eta}_q^{\mathrm{T}}\boldsymbol{R}_q(\xi\boldsymbol{I} - \boldsymbol{H}_q)\tilde{\boldsymbol{q}} > 0$.

Employing Young's inequality, we have

$$\begin{aligned} \boldsymbol{x}^{\mathrm{T}}\boldsymbol{f}_q &= \sqrt{\frac{16\lambda_{\min}(\boldsymbol{k}_x)}{(1+\delta)^2 l_{\alpha x}^2}}\boldsymbol{x}^{\mathrm{T}} \cdot \sqrt{\frac{(1+\delta)^2 l_{\alpha x}^2}{16\lambda_{\min}(\boldsymbol{k}_x)}}\boldsymbol{f}_q \\ &\le \frac{1}{2}\cdot\frac{16\lambda_{\min}(\boldsymbol{k}_x)}{(1+\delta)^2 l_{\alpha x}^2}\boldsymbol{x}^{\mathrm{T}}\boldsymbol{x} + \frac{1}{2}\cdot\frac{(1+\delta)^2 l_{\alpha x}^2}{16\lambda_{\min}(\boldsymbol{k}_x)} l_{fq}^2 \end{aligned} \tag{40}$$

where $l_{\alpha x} = \max_i \alpha_{xi}$.

Owing to the properties of the error transformation mapping Eq.(8), one obtains

$$\begin{aligned} -\boldsymbol{x}^{\mathrm{T}}\boldsymbol{k}_x\boldsymbol{R}_x\boldsymbol{\eta}_x &\le -\boldsymbol{x}^{\mathrm{T}}\boldsymbol{k}_x\lambda_{\min}(\boldsymbol{R}_x^{\mathrm{T}}\boldsymbol{R})\boldsymbol{\eta}_x \\ &\le -\frac{4}{(1+\delta)l_{\alpha x}}\boldsymbol{x}^{\mathrm{T}}\boldsymbol{k}_x\boldsymbol{\rho}(\theta_x)\cdot\frac{\boldsymbol{x}}{\boldsymbol{\alpha}_x} \\ &\le -\frac{4}{(1+\delta)l_{\alpha x}}\cdot\frac{4}{(1+\delta)l_{\alpha x}}\boldsymbol{x}^{\mathrm{T}}\boldsymbol{k}_x\boldsymbol{x} \\ &\le -\frac{16\lambda_{\min}(\boldsymbol{k}_x)}{(1+\delta)^2 l_{\alpha x}^2}\boldsymbol{x}^{\mathrm{T}}\boldsymbol{x}, \end{aligned} \tag{41}$$

$$\begin{aligned} -\boldsymbol{\eta}_q^{\mathrm{T}}\boldsymbol{e}_{est} - \tilde{\boldsymbol{q}}^{\mathrm{T}}\boldsymbol{R}_q\boldsymbol{e}_{est} &\le -\boldsymbol{e}_{est}^{\mathrm{T}}\frac{\boldsymbol{\rho}(\theta_q)}{\boldsymbol{\alpha}_q}\tilde{\boldsymbol{q}} - \tilde{\boldsymbol{q}}^{\mathrm{T}}\lambda_{\min}(\boldsymbol{R}_q^2)\boldsymbol{e}_{est} \\ &\le -\frac{8}{(1+\delta)l_{\alpha x}}\tilde{\boldsymbol{q}}^{\mathrm{T}}\boldsymbol{e}_{est} \end{aligned} \tag{42}$$

where

$\boldsymbol{\rho}(\boldsymbol{\theta}_q) = \mathrm{diag}([\rho(\theta_{q1}),\cdots,\rho(\theta_{q6})]^{\mathrm{T}})$,

$\boldsymbol{\rho}(\boldsymbol{\theta}_x) = \mathrm{diag}([\rho(\theta_{x1}),\cdots,\rho(\theta_{x6})]^{\mathrm{T}})$.

Substituting (40)-(41) into (39) yields

$$\begin{aligned} \dot{V}_1 &\le \frac{1}{2}\cdot\frac{16\lambda_{\min}(\boldsymbol{k}_x)}{(1+\delta)^2 l_{\alpha x}^2}\boldsymbol{x}^{\mathrm{T}}\boldsymbol{x} + \frac{1}{2}\cdot\frac{(1+\delta)^2 l_{\alpha x}^2}{16\lambda_{\min}(\boldsymbol{k}_x)} l_{fq}^2 \\ &\quad -\frac{16\lambda_{\min}(\boldsymbol{k}_x)}{(1+\delta)^2 l_{\alpha x}^2}\boldsymbol{x}^{\mathrm{T}}\boldsymbol{x} - \xi\boldsymbol{\eta}_q^{\mathrm{T}}\tilde{\boldsymbol{q}} - \frac{8}{(1+\delta)l_{\alpha x}}\tilde{\boldsymbol{q}}^{\mathrm{T}}\boldsymbol{e}_{est} \\ &\le -\frac{16\lambda_{\min}(\boldsymbol{k}_x)}{(1+\delta)^2 l_{\alpha x}^2}\cdot\frac{1}{2}\boldsymbol{x}^{\mathrm{T}}\frac{\boldsymbol{D}}{\|\boldsymbol{D}\|}\boldsymbol{x} - \xi\boldsymbol{\eta}_q^{\mathrm{T}}\tilde{\boldsymbol{q}} \\ &\quad +(\frac{1}{2}\cdot\frac{(1+\delta)^2 l_{\alpha x}^2 l_{fq}^2}{16\lambda_{\min}(\boldsymbol{k}_x)} - \frac{8}{(1+\delta)l_{\alpha x}}\tilde{\boldsymbol{q}}^{\mathrm{T}}\boldsymbol{e}_{est}) \\ &\le -\frac{16\lambda_{\min}(\boldsymbol{k}_x)}{(1+\delta)^2 l_{\alpha x}^2\lambda_{\max}(\boldsymbol{D})}\cdot\frac{1}{2}\boldsymbol{x}^{\mathrm{T}}\boldsymbol{D}\boldsymbol{x} - \xi\boldsymbol{\eta}_q^{\mathrm{T}}\tilde{\boldsymbol{q}} \\ &\quad +(\frac{(1+\delta)^2 l_{\alpha x}^2 l_{fq}^2}{32\lambda_{\min}(\boldsymbol{k}_x)} - \frac{8\tilde{\boldsymbol{q}}^{\mathrm{T}}\boldsymbol{e}_{est}}{(1+\delta)l_{\alpha x}}). \end{aligned} \tag{43}$$

Define

$$c_{12} = \frac{(1+\delta)^2 l_{\alpha x}^2 l_{fq}^2}{32\lambda_{\min}(\boldsymbol{k}_x)} - \frac{8\tilde{\boldsymbol{q}}^{\mathrm{T}}\boldsymbol{e}_{est}}{(1+\delta)l_{\alpha x}}$$

which is a bounded constant on account of the boundedness of $\tilde{\boldsymbol{q}}$ and $\boldsymbol{e}_{est}$. Thus, there exists a constant

$$c_{11} = \min\left(\frac{16\lambda_{\min}(\boldsymbol{k}_x)}{(1+\delta)^2 l_{\alpha x}^2\lambda_{\max}(\boldsymbol{D})}, \xi\right)$$

such that

$$\dot{V}_1 \le -c_{11}V_1 + c_{12} . \tag{44}$$

Integrating (44) yields

$$\begin{aligned} V_1(t) &\le V_1(0)e^{-c_{11}t} + \frac{c_{12}}{c_{11}}(1-e^{-c_{11}t}) \\ &\le V_1(0) + \frac{c_{12}}{c_{11}}. \end{aligned} \tag{45}$$

The boundedness of V_1 in (45) indicates that $\boldsymbol{\eta}_q$ is bounded when $t \in [0, t_f)$.

For the boundedness of $\boldsymbol{\eta}_x$, assign a Lyapunov function

$$V_2 = \frac{1}{2}\boldsymbol{\eta}_x^{\mathrm{T}}\boldsymbol{k}_x\boldsymbol{\eta}_x . \tag{46}$$

Similar to the previous step, the derivative of V_2 along Eq.(2) satisfies

$$\begin{aligned} \dot{V}_2 &= \boldsymbol{\eta}_x^{\mathrm{T}}\boldsymbol{k}_x\boldsymbol{R}_x\boldsymbol{D}^{-1}(\boldsymbol{D}\dot{\boldsymbol{x}} + \boldsymbol{D}\boldsymbol{H}_x\boldsymbol{x}) \\ &= \boldsymbol{\eta}_x^{\mathrm{T}}\boldsymbol{k}_x\boldsymbol{R}_x\boldsymbol{D}^{-1}(\xi\boldsymbol{D}\tilde{\boldsymbol{q}} + \boldsymbol{D}\dot{\boldsymbol{e}}_{est} - \boldsymbol{D}\ddot{\boldsymbol{q}}_r - \boldsymbol{C}\dot{\boldsymbol{q}}_r \\ &\quad -\boldsymbol{C}\dot{\tilde{\boldsymbol{q}}} + \boldsymbol{\tau} + \boldsymbol{D}\boldsymbol{H}_x\boldsymbol{x}) \\ &= \boldsymbol{\eta}_x^{\mathrm{T}}\boldsymbol{k}_x\boldsymbol{R}_x\boldsymbol{D}^{-1}(\boldsymbol{f}_q + \boldsymbol{f}_x) - \boldsymbol{\eta}_x^{\mathrm{T}}\boldsymbol{k}_x\boldsymbol{R}_x\boldsymbol{D}^{-1}\boldsymbol{k}_x\boldsymbol{R}_x\boldsymbol{\eta}_x \end{aligned} \tag{47}$$

where $\boldsymbol{f}_x = -\boldsymbol{C}\boldsymbol{x} - \boldsymbol{R}_q\tilde{\boldsymbol{q}} - \boldsymbol{\eta}_q + \boldsymbol{D}\boldsymbol{H}_x\boldsymbol{x}$. $\boldsymbol{\eta}_q$ has been proven to be bounded and thus $\boldsymbol{R}_q$ is bounded as well. $\tilde{\boldsymbol{q}}$ and $\boldsymbol{x}$ satisfy their boundary constraints and $\boldsymbol{H}_x$ is bounded when $t \in [0, t_f)$. Recalling Lemma 1, we can state that there exists a constant $l_{fx} \ge 0$ as well such that

$$\left\| \boldsymbol{f}_x \right\| \le l_{fx} . \tag{48}$$

Then employing Young's inequality and the properties of the error transformation mapping Eq.(8) yields that

$$\begin{aligned} \dot{V}_2 &= \boldsymbol{\eta}_x^{\mathrm{T}}\boldsymbol{k}_x\boldsymbol{R}_x\boldsymbol{D}^{-1}(\boldsymbol{f}_q + \boldsymbol{f}_x) - \boldsymbol{\eta}_x^{\mathrm{T}}\boldsymbol{k}_x\boldsymbol{R}_x\boldsymbol{D}^{-1}\boldsymbol{k}_x\boldsymbol{R}_x\boldsymbol{\eta}_x \\ &\le \frac{\boldsymbol{k}_x\boldsymbol{R}_x\boldsymbol{\eta}_x\sqrt{\lambda_{\max}(\boldsymbol{D})}}{\sqrt{\lambda_{\max}(\boldsymbol{D})}}\boldsymbol{D}^{-1}(\boldsymbol{f}_q + \boldsymbol{f}_x) - \frac{\|\boldsymbol{k}_x\boldsymbol{R}_x\boldsymbol{\eta}_x\|^2}{\lambda_{\max}(\boldsymbol{D})} \\ &\le \frac{\lambda_{\max}(\boldsymbol{D})}{2}\|\boldsymbol{D}^{-1}\|^2\|\boldsymbol{f}_q + \boldsymbol{f}_x\|^2 - \frac{\|\boldsymbol{k}_x\boldsymbol{R}_x\boldsymbol{\eta}_x\|^2}{2\lambda_{\max}(\boldsymbol{D})} \\ &\le \frac{\lambda_{\max}(\boldsymbol{D})(l_{fq} + l_{fx})^2}{(\lambda_{\min}(\boldsymbol{D}))^2} - \frac{16\lambda_{\min}(\boldsymbol{k}_x)}{\lambda_{\max}(\boldsymbol{D})(1+\delta)^2 l_{\alpha x}^2}V_2. \end{aligned} \tag{49}$$

Apparently, there exist two constants

$$c_{21} = \frac{16\lambda_{\min}(\boldsymbol{k}_x)}{\lambda_{\max}(\boldsymbol{D})(1+\delta)^2 l_{\alpha x}^2},$$

$$c_{22} = \frac{\lambda_{\max}(\boldsymbol{D})(l_{fq} + l_{fx})^2}{(\lambda_{\min}(\boldsymbol{D}))^2}$$

such that

$$\dot{V}_2 \le -c_{21}V_2 + c_{22} . \tag{50}$$

Similarly to the previous proof, one can obtain that

V_2 and $\boldsymbol{\eta}_x$ are both bounded during the time interval $[0, t_f)$.

Finally, we will prove that the boundary constraints for $\tilde{\boldsymbol{q}}(t)$ and $\boldsymbol{x}(t)$ always hold for $t \geq 0$.

In the previous steps, we get that $\boldsymbol{\eta}(t) = [\boldsymbol{\eta}_q^{\mathrm{T}}(t), \boldsymbol{\eta}_x^{\mathrm{T}}(t)]^{\mathrm{T}}$ is bounded, i.e. $\|\boldsymbol{\eta}(t)\|_\infty \leq l_\eta$ when $t \in [0, t_f)$, where l_η is a bounded constant. Recalling Eq.(14), we can find a compact set $[\mu^{-1}(-l_\eta), \mu^{-1}(l_\eta)]$ for each $D_{\theta i}$ such that $\theta_i(t)$ is within the compact set when $t \in [0, t_f)$. From Proposition C.3.6 in [37], we get $t_f = +\infty$, i.e. the prescribed performance boundary constraints for $\tilde{\boldsymbol{q}}(t)$ and $\boldsymbol{x}(t)$ always hold for all $t \geq 0$. Thus restrained by the prescribed-time prescribed-performance functions, $\tilde{\boldsymbol{q}}(t)$ and $\boldsymbol{x}(t)$ converge to the stability regions in Eqs.(30) and (31) before the prescribed time T.

Based on Eq.(32), the joint angular velocity errors $\dot{\tilde{\boldsymbol{q}}}$ remains bounded for $t \geq 0$ as well.

The control objectives are all achieved. This is the end of proof. □

Remark 2: The prescribed time T can be pre-specified theoretically to a sufficiently small value. However, the control inputs are always limited when the specific actuators are considered in practical space missions. Therefore the actuator saturation problem may be encountered. It should be noted that fast convergence speed is based on large control inputs, which may not be realized for actual manipulator control systems. Consequently, a reasonable T should be designed on the basis of the requirements and actuator's ability.

4. SIMULATION ANALYSIS

To illustrate the performance of the proposed PTPPC control scheme, the system dynamics (2) are propagated by adopting controller Eq.(29). The spacecraft base attitude is controlled by a simple PD controller to remain at its initial state. The influence of the spacecraft base attitude and external disturbance are both taken into consideration. The mass of the spacecraft base is 200kg and the its inertia is $\mathrm{diag}([30, 30, 30]^{\mathrm{T}})\ \mathrm{kg \cdot m^2}$. The mass and length of each link is as follow: $m_1 = m_4 = m_5 = m_6 = 1.2$ kg, $m_2 = m_3 = 6.5$ kg, $l_1 = l_4 = l_5 = l_6 = 0.2$ m, $l_2 = l_3 = 1.8$ m. The total simulation time is 40s and the prescribed time is preassigned as 20s. The initial conditions of the spacecraft base attitude and manipulator joint angles are set as $\boldsymbol{\Phi} = \boldsymbol{0}$ and $\boldsymbol{q}(0) = \dot{\boldsymbol{q}}(0) = \boldsymbol{0}$, respectively. The reference signals of the joint angles are set as $\boldsymbol{q}_r = [30^\circ, 30^\circ, 30^\circ, 10^\circ, 30^\circ, 15^\circ]^{\mathrm{T}}$ and $\dot{\boldsymbol{q}}_r = \boldsymbol{0}$. A sinusoidal external disturbance of peak amplitude equal to $0.1\ \mathrm{N \cdot m}$ is exerted on the whole system. The control parameters are set as follows: $\alpha_{qi}^0 = 1.32$, $\alpha_{qi}^T = 0.01$, $\alpha_{xi}^0 = 1.72$, $\alpha_{xi}^T = 0.1$, $\gamma = 0.8$, $\delta = 0.9$, $\xi = 0.6$, $\boldsymbol{k} = \mathrm{diag}([3, 25, 6, 8, 25, 5]^{\mathrm{T}})$, $p_0 = p_1 = p_2 = 18$, $s_1 = s_2 = 9$.

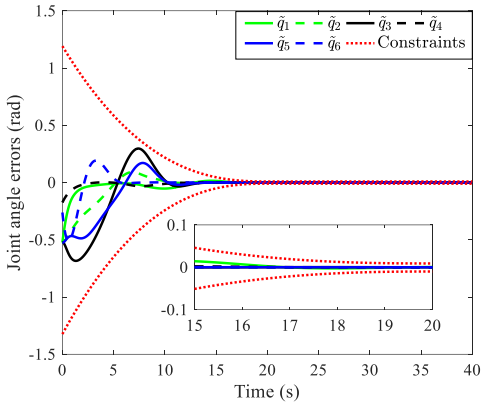

Fig. 4. Time histories of joint angle errors.

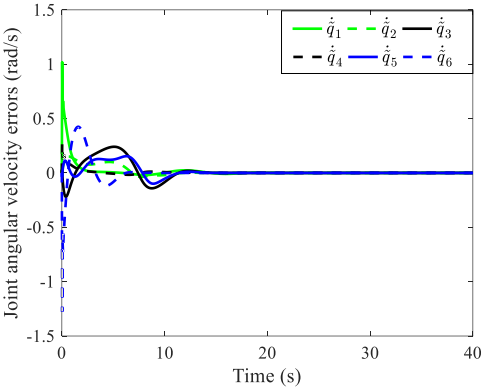

Fig. 5. Time histories of joint angular velocity errors.

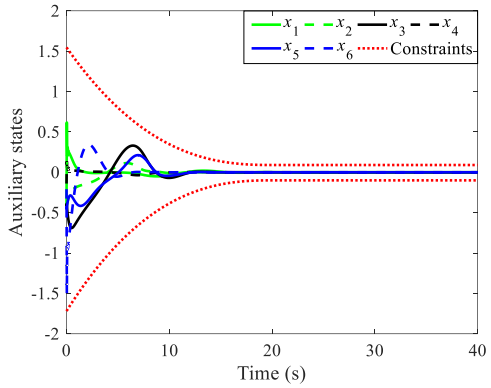

Fig. 6. Time histories of auxiliary states.

Figs. 4-6 depict the joint angles, angular velocities and auxiliary states, which all satisfy their boundary constraints and converge to prescribed stability domains before the predefined settling time $T = 20$s in the presence of external disturbances. It can be observed from the subgraph of Fig. 4 that the steady-state errors of joint angles converge to their prescribed stability domains effectively and are always within the boundaries. In the entire control process, the proposed TD obtains a great tracking with a rapid transition and the estimation errors converge to zero after a short oscillation, as shown in Fig. 8, which illustrates the prescribed-time stability

with prescribed performance and the robustness of the proposed controller. Fig. 7 shows the time histories of the control torques applied to the joints. The time histories of actual motion of the spacecraft base attitude and corresponding control torques are plotted in Fig. 9 and Fig. 10, respectively, from which one can observe that the spacecraft base attitude experiences a slight oscillation during the initial stage but returns to stability rapidly under the contoller.

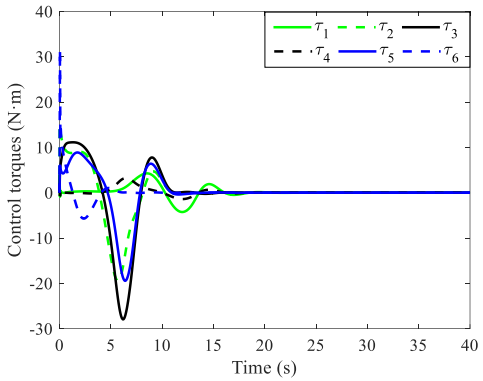

Fig. 7. Time histories of control torques for joints.

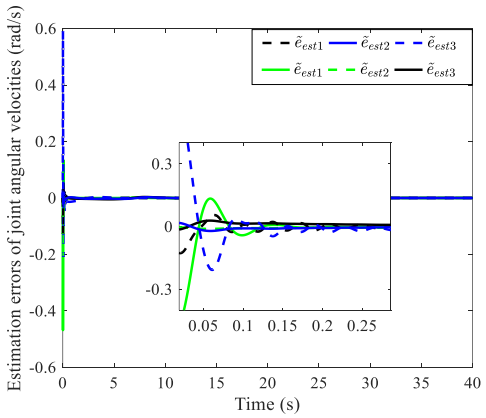

Fig. 8. Time histories of estimation errors of joint angular velocities.

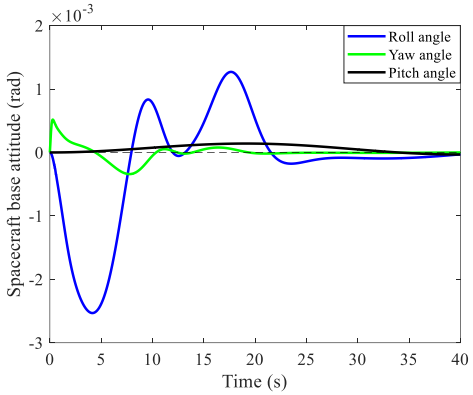

Fig. 9. Time histories of spacecraft base attitude.

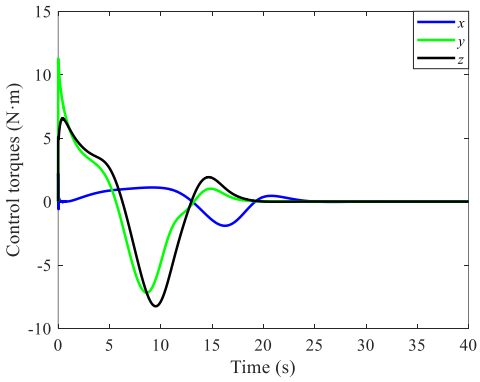

Fig. 10. Time histories of control torques for spacecraft base attitude.

To illustrate the influence of the spacecraft base attitude and external disturbance to the space manipulator, a simulation is carried out without the spacecraft base attitude controller and external disturbance. The time histories of joint angle errors and corresponding control torques are plotted in Fig. 11 and Fig. 12. Comparing with Fig. 4 and Fig. 7, it is obviously that the spacecraft base attitude and external disturbance resulted in larger overshoot of joint angle errors and increasing of control torques but joint angles satisfy their boundary constraints and converge to prescribed stability domains before the predefined settling time $T = 20\text{s}$ nevertheless.

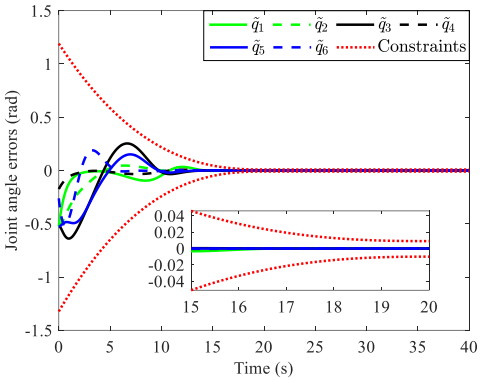

Fig. 11. Time histories of joint angle errors.

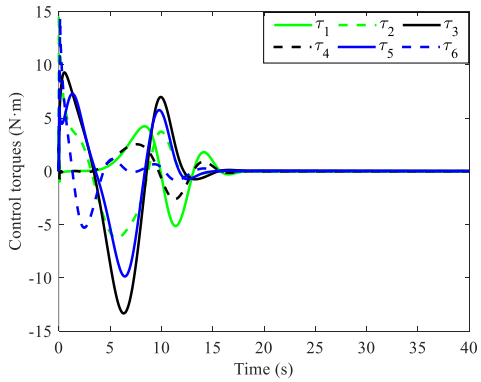

Fig. 12. Time histories of control torques for joints.

Simulating in the same scenario except the prescribed time is set as $T = 30\text{s}$, one can obtain the time histories of joint angles as shown in Fig. 13, where the system

states experience a longer transient process but all converge to a desired small neighbourhood around the origin with the prescribed performance before 30s and remain in the stability domains. Given that the prescribed time is independent of the system condition, it can be predesigned off-line by user in accordance with mission requirements. Fig. 14 shows the time evolution of control torques during the whole process. Comparing with Fig. 7, it is observed that the shorter prescribed settling time in general requires larger control inputs. Therefore, although the prescribed time T can be preassigned theoretically to a sufficiently small value, it is necessary to design it in the light of both mission requirements and the capability of actuators because an unreasonable one may bring actuator saturation problems in practical application.

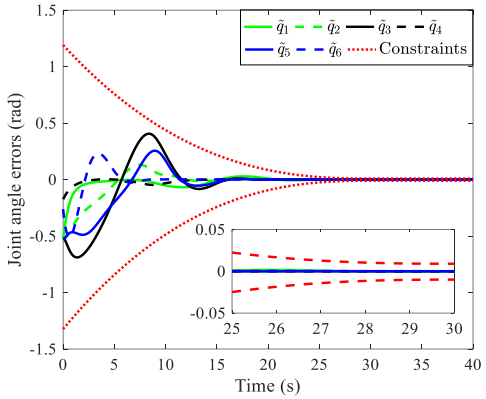

Fig. 13. Time histories of joint angle errors when T = 30s.

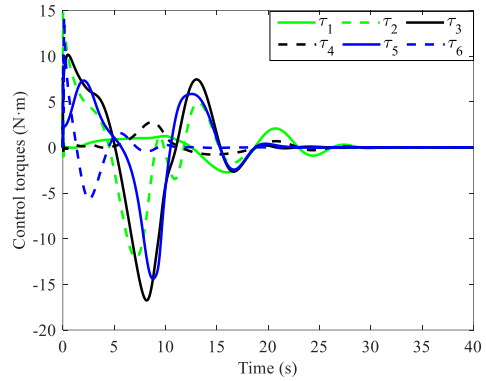

Fig. 14. Time histories of control torques for joints when T = 30s.

Time-varying reference signals are set to verify the tracking capability of the proposed control scheme. The reference signals of joint angles are given by

$$\begin{cases} q_{r1} = -q_{r2} = 0.436\sin(0.025\pi t + 0.5\pi) + 0.436 \\ q_{r3} = -q_{r4} = 0.262\sin(0.025\pi t + 0.5\pi) + 0.262 \\ q_{r5} = -q_{r6} = 0.175\sin(0.025\pi t + 0.5\pi) + 0.175. \end{cases} \quad (51)$$

To simulate a challenging scenario, the parameters related to performance functions are set as $\alpha_{qi}^{0} = 0.1$, $\alpha_{qi}^{T} = 0.01$, $\alpha_{xi}^{0} = 0.5$, $\alpha_{xi}^{T} = 0.01$ and the prescribed time is set as $T = 10\text{s}$, while other design parameters are set as the same as the preceding scenario.

Fig. 15 displays the time histories of joint angles, from which one can conclude that the joint angles converge to the desired joint angles rapidly before the prescribed time T and then highly precise tracking performance can be obtained. The joint angular velocities, as shown in Fig. 16, converge to the user-defined stable regions, residing in the time-varying boundaries before the prescribed time T and the steady-state performances are excellent as well.

The tracking performances and errors of joint angular velocities are given in Fig. 17. Notice that the proposed TD can provide a satisfactory tracking of the joint angular velocities with a rapid transition, and the tracking errors remain very small during the entire control process and can converge to zero in finite time.

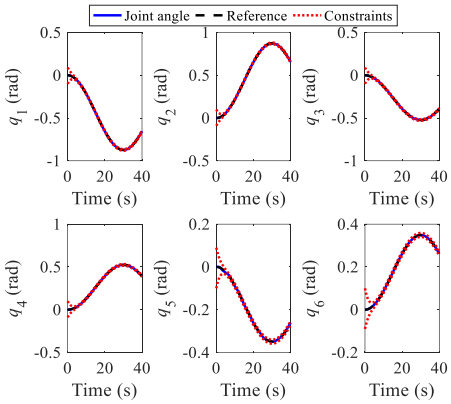

Fig. 15. Joint angles tracking performances.

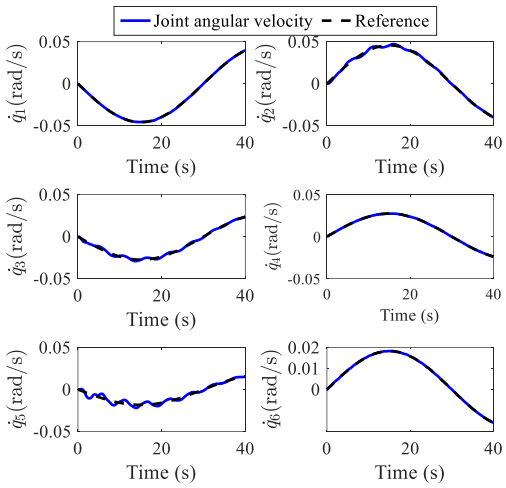

Fig. 16. Joint angular velocities tracking performances.

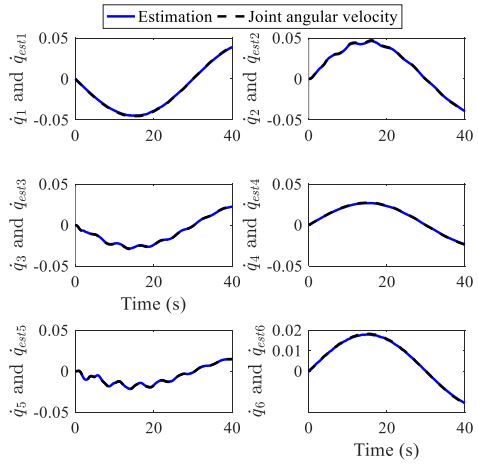

Fig. 17. Time histories of joint angular velocities and their estimations.

In order to illustrate the superiority of the proposed controller, a traditional prescribed performance controller, imposing an exponentially decaying performance function in the form of Eq.(52) on the auxiliary state, for the space manipulator system is designed as well and simulated in the same scenario. The responses of each state are shown in Figs. 18-20.

$$\alpha(t) = (\alpha^0 - \alpha^\infty)e^{-\beta t} + \alpha^\infty,\ (\alpha^0 > \alpha^\infty > 0) \qquad (52)$$

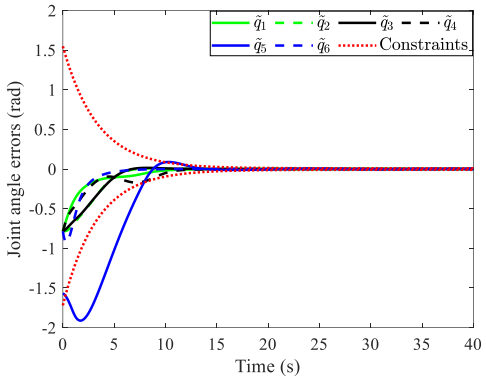

Fig. 18. Time histories of joint angle errors (under traditional prescribed performance control).

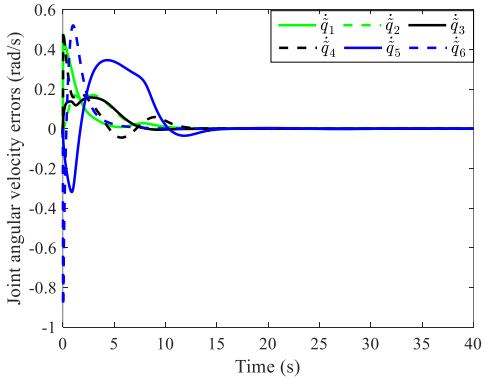

Fig. 19. Time histories of joint angular velocity errors (under traditional prescribed performance control).

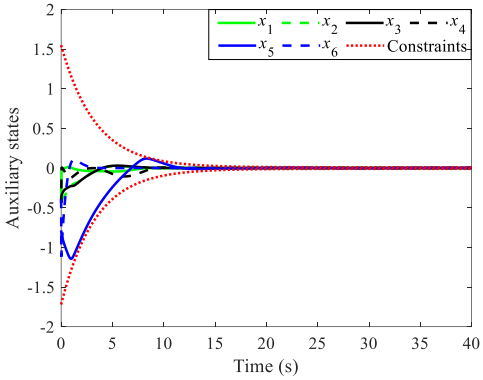

Fig. 20. Time histories of auxiliary states (under traditional prescribed performance control).

In comparison with Figs. 4-6, all states under the traditional prescribed performance control apparently experience a severer oscillation in transient stage. In addition, the traditional prescribed performance controller only guarantees the auxiliary state rather than all states to converge within the prescribed boundary constraints, which may cause that some states cross their practical boundary constraints, such as $\tilde{q}_5$ in Fig. 14. This is a failure prescribed performance control. Moreover, to achieve a satisfactory settling time, a tedious regulation of the controller parameters is a necessity for the traditional prescribed performance control, while the user can pre-assign the settling time based on the mission requirement in the proposed PTPPC.

5. CONCLUSION

A low-complexity prescribed performance controller guaranteeing both settling time and prescribed control performance is proposed for motion tracking control of a space manipulator in this paper. Compared with the traditional perescribed performance control baed on exponentially decaying performance functions, the proposed PTPPC control scheme not only guarantees the system transient and steady-state control performances satisfy the prescribed boundary constraints, but also confines all tracking errors to converge to stability domains before the user-defined settling time. To lower hardware requirements for the controlled system to a certain extent, a nonlinear tracking differentiator based on a hyperbolic sine function is adopted to estimate the derivatives of joint angles and reconstruct the angular velocity for the controller. Without time-consuming operations and model information, the proposed contriller has a superiority in low computation complexity and robustness against model uncertainties. Moreover, selecting the control gains is no longer a lengthy and gruelling task because adjusting them to generate reasonable input torques is the only consideration. Numerical simulation and the comparison with the traditional prescribed performance controller demonstrates the effectiveness and superior performances of the proposed control scheme.

REFERENCES

[1] T. Zhang, M. H. Zhang, and Y. B. Zou, "Time-optimal and smooth trajectory planning for robot manipulators," *International Journal of Control, Automation and Systems*, vol. 19, no. 1, pp. 521-531, March 2020.

[2] F. Aghili, "Optimal trajectories and robot control for detumbling a non-cooperative satellite," *Journal of Guidance Control and Dynamics*, vol. 43, no. 5, pp. 981-987, May 2020.

[3] P. F. Huang, M. Wang, Z. J. Meng, F. Zhang, and Z. X. Liu, "Attitude takeover control for post-capture of target spacecraft using space robot," *Aerospace Science and Technology*, vol. 51, pp. 171-180, February, 2016.

[4] Y. Mo, Z. H. Jiang, H. Li, H. Yang, and Q. Huang, "A novel space target-tracking method based on generalized Gaussian distribution for on-orbit maintenance robot in Tiangong-2 space laboratory," *Science China Technological Sciences*, vol. 62, pp. 1045-1054, June 2019.

[5] X. L. Ding, Y. C. Wang, Y. B. Wang, and K. Xu, "A review of structures, verification, and calibration technologies of space robotic systems for on-orbit servicing," *Science China Technological Sciences*, vol. 64, pp. 462-480, March 2021.

[6] F. Han and Y. Jia, "Sliding mode boundary control for a planar two-link rigid-flexible manipulator with input disturbances," *International Journal of Control, Automation and Systems*, vol. 18, pp. 351-362, February 2020.

[7] M. Homayounzade and A. Khademhosseini, "Disturbance observer-based trajectory following control of robot manipulators," *International Journal of Control, Automation and Systems*, vol. 17, pp. 203-211, January 2019.

[8] R. Koningstein and R. H. Jr. Cannon, "Experiments with model-simplified computed-torque manipulator controllers for free-flying robots," *Journal of Guidance Control and Dynamics*, vol. 18, no. 6, pp. 1386-1391, November-December 1995.

[9] H. Berghuis and H. Nijmeijer, "A passivity approach to controller-observer design for robots," *IEEE Trans. on Robotics and Automation*, vol. 9, no. 6, pp. 740-754, December 1993.

[10] Z. Yu, X. Liu, and G. Cai, "Dynamics modeling and control of a 6-DOF space robot with flexible panels for capturing a free floating target," *Acta Astronautica*, vol. 128, pp. 560-572, August 2016.

[11] A. Seddaoui and C. M. Saaj, "Combined nonlinear H_∞ controller for a controlled-floating space robot," *Journal of Guidance Control and Dynamics*, vol. 42, no. 8, pp. 1878-1885, August 2019.

[12] S. Soumya and K.R. Guruprasad, "Model-based, distributed, and cooperative control of planar serial-link manipulators," *International Journal of Control, Automation and Systems*, vol. 19, pp. 850-863, February 2021.

[13] S. Jung, "A neural network technique of compensating for an inertia model error in a time-delayed controller for robot manipulators," *International Journal of Control, Automation and Systems*, vol. 18, pp. 1863-1871, February 2020.

[14] A. Ailon and R. Ortega, "An observer-based set-point controller for robot manipulators with flexible joints," *Systems & Control Letters*, vol. 21, no. 4, pp. 329-335, October 1993.

[15] R. Ortega R, A. Loría A, and R. Kelly, "A semiglobally stable output feedback PI^2D regulator for robot manipulators," *IEEE Trans. on Automatic Control*, vol. 40, no. 8, pp. 1432-1436, August 1995.

[16] S. P. Liu, L. C. Wu, and Z. Lu, "Impact dynamics and control of a flexible dual-arm space robot capturing an object," *Applied Mathematics and Computation*, vol. 185, pp. 1149-1159, 2007.

[17] S. Kawamura, F. Miyazaki, and S. Arimoto, "Is a local linear PD feedback control law effective for trajectory tracking of robot motion?" *Proc. of International Conf. Robotics and Automation*, pp. 1335-1340, 1988.

[18] Z. H. Qu, D. M. Dawson, J. F. Dorsey, and J. D. Duffie, "Robust estimation and control of robotic manipulators," *Robotica*, vol. 13, no. 3, pp. 223-231, July 1995.

[19] R. Kelly, "A tuning procedure for stable PID control of robot manipulators," *Robotica*, vol. 13, no. 2, pp. 141-148, May 1995.

[20] Y. Cao and C. W. Silva, "Dynamic modeling and neural-network adaptive control of a deployable manipulator system," *Journal of Guidance Control and Dynamics*, vol. 29, no. 1, pp. 192-194, January-February 2006.

[21] A. Green and J. Z. Sasiadek, "Adaptive control of a flexible robot using fuzzy logic," *Journal of Guidance Control and Dynamics*, vol. 28, no. 1, pp. 36-42, January-February 2005.

[22] H. Liu, H. R. Wang, S. W. Fan, and D. P. Yang, "Bio-inspired design of alternate rigid-flexible segments to improve the stiffness of a continuum manipulator," *Science China Technological Sciences*, vol. 63, pp. 1549-1559, August 2020.

[23] B. Xian, M. S. Queiroz, D. M. Dawson, and M. L. McIntyrea, "A discontinuous output feedback controller and velocity observer for nonlinear mechanical systems," *Automatica*, vol. 40, no. 4, pp. 695-700, 2004.

[24] Y. Su, P. C. Muller, and C. Zheng, "A simple nonlinear observer for a class of uncertain mechanical systems," *IEEE Trans. on Automatic Control*, vo. 52, no. 7, pp. 1340-1345, July 2007.

[25] M. Rognant, C. Cumer, J. M. Biannic, M. A. Roa, A. Verhaeghe, and V. Bissonnette, "Autonomous assembly of large structures in space: a technology review," *8th European Conf. Aeronautics and Aerospace Sciences*, pp. 1-13, 2019.

[26] C. P. Bechlioulis and G. A. Rovithakis, "Robust adaptive control of feedback linearizable MIMO nonlinear systems with prescribed performance," *IEEE Trans. on Automatic Control*, vol. 53, no. 9, pp. 2090-2099, October 2008.

[27] C. P. Bechlioulis and G. A. Rovithakis, "Adaptive control with guaranteed transient and steady state tracking error bounds for strict feedback systems," *Automatica*, vol. 45, no. 2, pp. 532-538, 2009.

[28] C. P. Bechlioulis and G. A. Rovithakis, "Prescribed performance adaptive control for multi-input multi-output affine in the control nonlinear systems," *IEEE Trans. on Automatic Control*, vol. 55, no. 5, pp. 1220-1226, May 2010.

[29] J. J. Luo, C. S. Wei, H. H. Dai, Z. Y. Yin, X. Wei, and J. P. Yuan, "Robust inertia-free attitude takeover control of postcapture combined spacecraft with guaranteed prescribed performance," *ISA Transactions*, vol. 74, pp. 28-44, January 2018.

[30] C. Bechlioulis, Z. Doulgeri, and G. Rovithakis, "Robot force/position tracking with guaranteed prescribed performance," *Proc. of International Conf. Robotics and Automation*, pp. 3688-3693, 2009.

[31] Z. Doulgeri, Y. Karayiannidis, and O. Zoidi, "Prescribed performance control for robot joint trajectory tracking under parametric and model uncertainties," *Proc. of 17th Mediterranean Conf. Control and Automation*, vol. 1, pp. 1313–1318, 2009.

[32] C. M. Hackl, C. Endisch, and D. Schröder, "Contributions

to nonidentifier based adaptive control in mechatronics," *Robotics and Autonomous Systems*, vol. 57, no. 10, pp. 996-1005, October 2009.

[33] Y. Karayiannidis, D. Papageorgiou, and Z. Doulgeri, "A model-free controller for guaranteed prescribed performance tracking of both robot joint positions and velocities," *IEEE Robotics and Automation Letters*, vol. 1, no. 1, pp. 267-273, January 2016.

[34] M. W. Spong, S. Hutchinson, and M. Vidyasagar, *Robot dynamics and control*, 2nd ed, John Wiley & Sons, New Jersey, USA, 2004.

[35] Y. X. Su, C. H. Zheng, D. Sun, and B. Y. Duan, "A simple nonlinear velocity estimator for high-performance motion control," *IEEE Trans. on Industrial Electronics*, vol. 52, no. 4, pp. 1161-1169, August 2005.

[36] H. K. Khalil, *Nonlinear Systems*, 3rd ed, Prentice-Hall, New Jersey, USA, 2002.

[37] E. D. Sontag, *Mathematical control theory: deterministic finite dimensional systems*, 2nd ed, Springer-Verlag, New York, 1998.